

Supplementary Information

Proton donor modulating ESIPT-based fluorescent probes for highly sensitive and selective detection of Cu²⁺

*Liyan Huang, Biao Gu, Wei Su, Peng Yin, Haitao Li**

Key Laboratory of Chemical Biology and Traditional Chinese Medicine Research (Ministry of Education), College of Chemistry and Chemical Engineering, Hunan Normal University, Changsha 410081, PR China

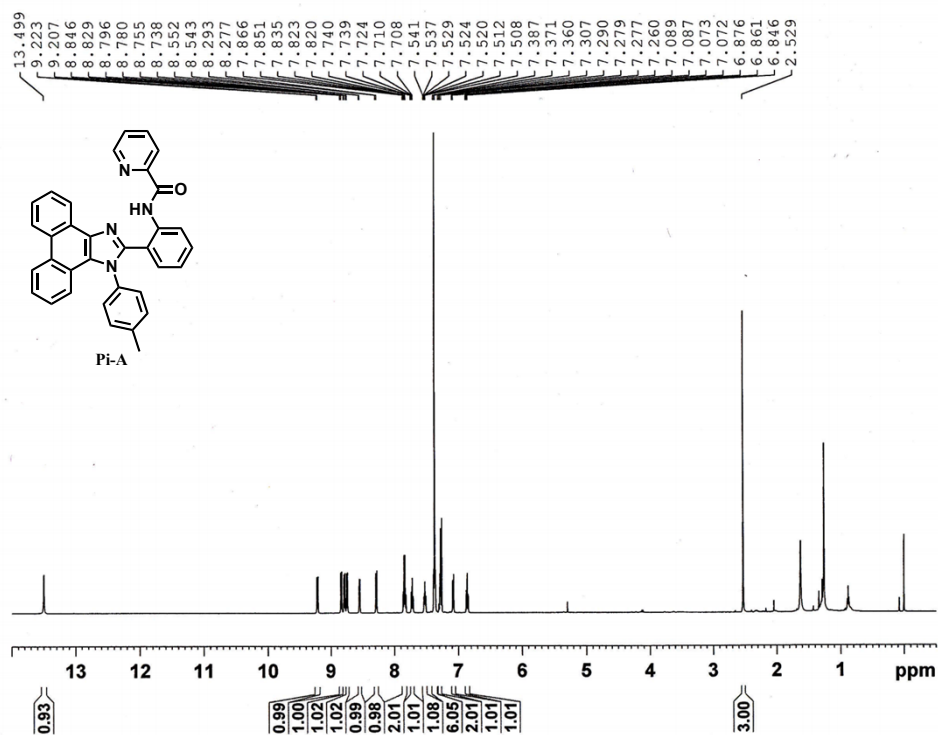


Fig. S1. ¹H NMR spectrum of Pi-A (500 MHz, CDCl₃).

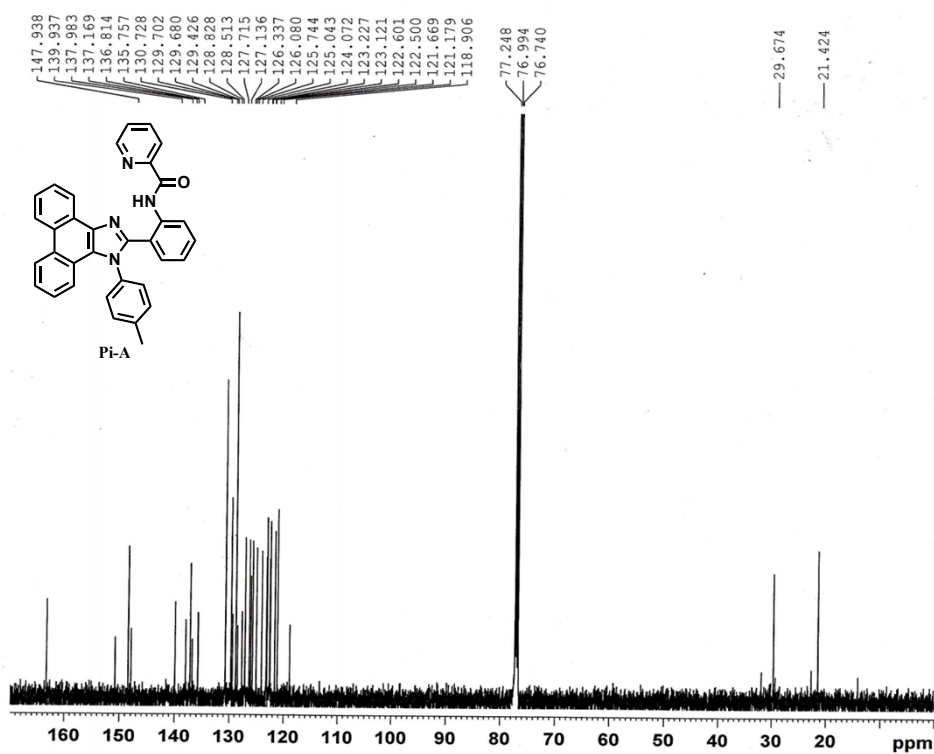


Fig. S2. ¹³C NMR spectrum of Pi-A (126 MHz, CDCl₃).

20150108GU 165 (1.663) Cm (132:216)

Scan ES+
3.38e6

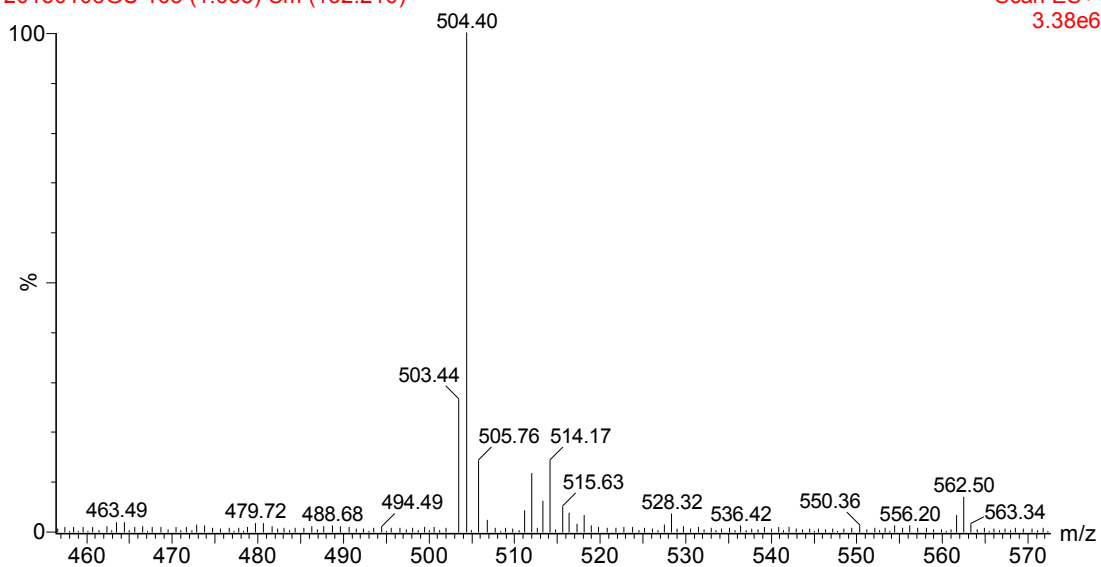


Fig. S3. ESI-MS spectrum of Pi-A.

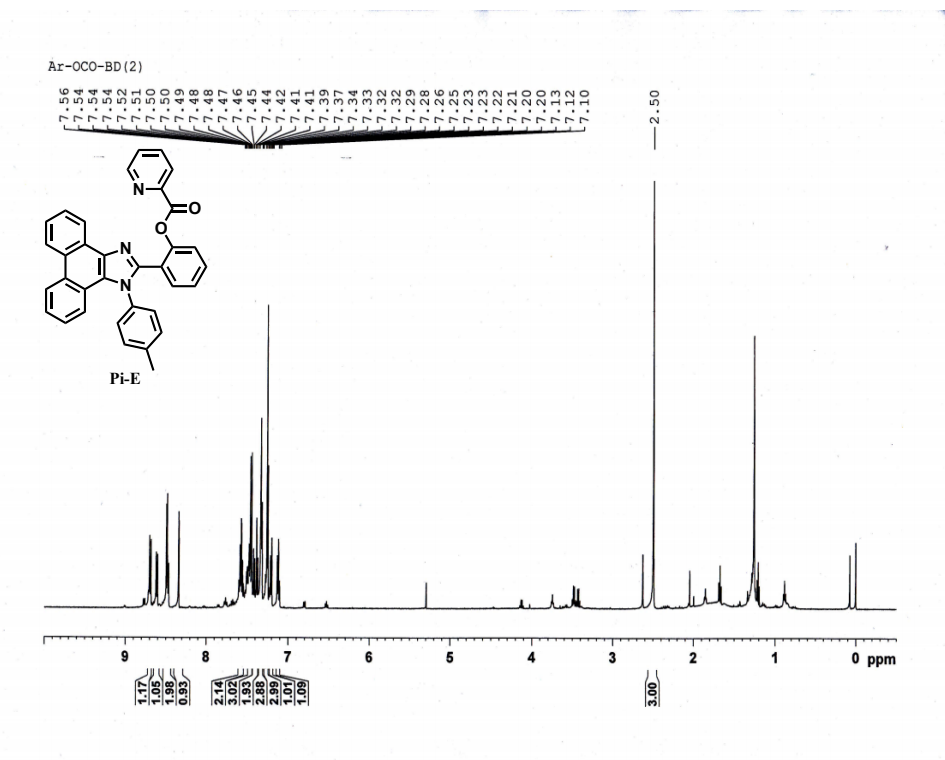


Fig. S4. ¹H NMR spectrum of Pi-E (500 MHz, CDCl₃).

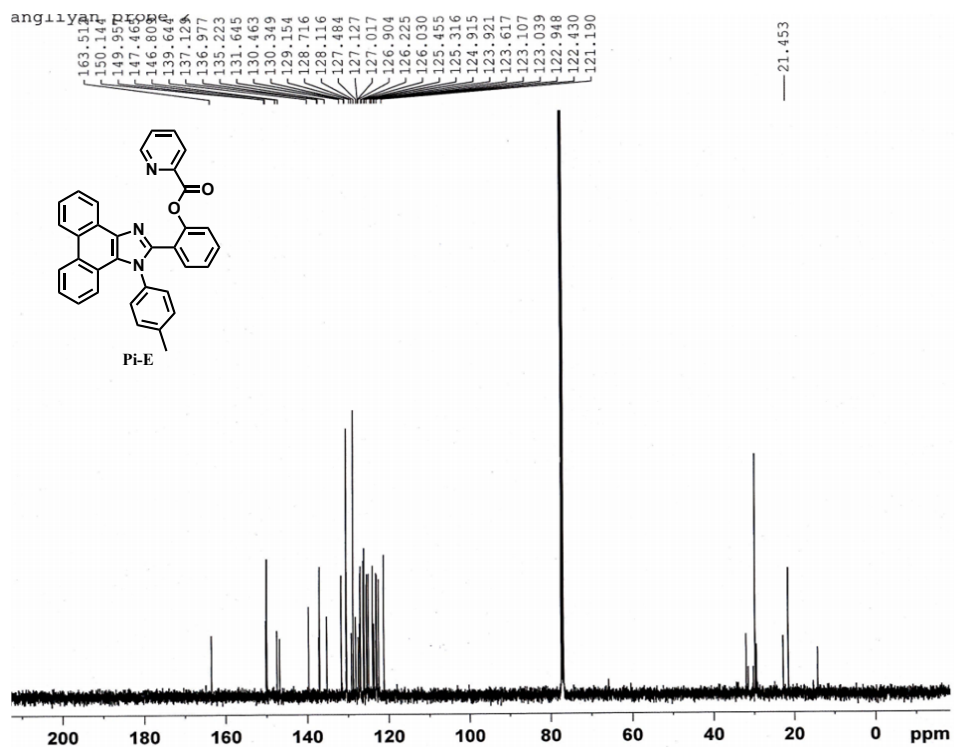


Fig. S5. ^{13}C NMR spectrum of Pi-E (126 MHz, CDCl_3).

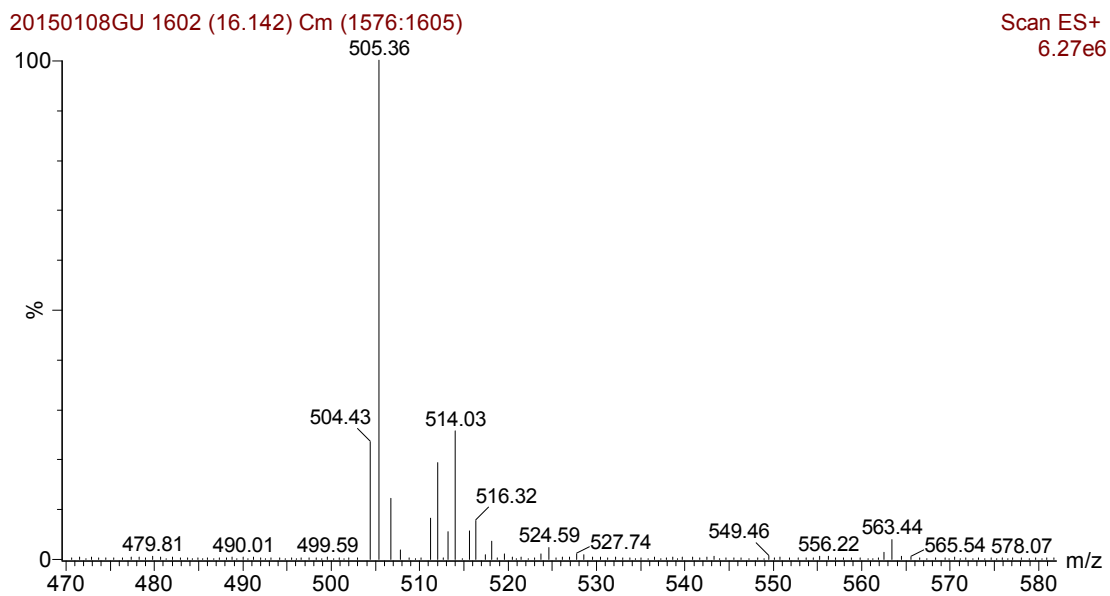


Fig. S6. ESI-MS spectrum of Pi-E.

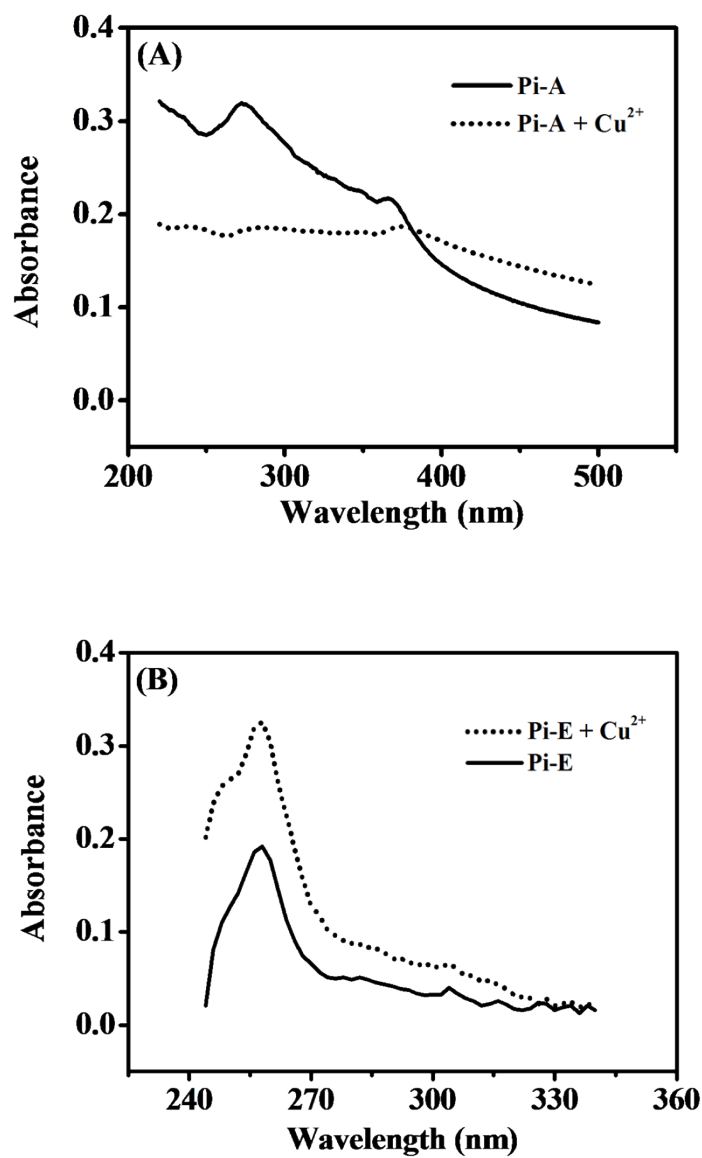


Fig. S7. Absorption spectra of 10 μM Pi-A (A) and Pi-E (B) in the absence and presence of 10 μM Cu^{2+} . Buffer: Tris-HCl (10 mM, pH 7.4), 2% (v/v) DMSO/water.

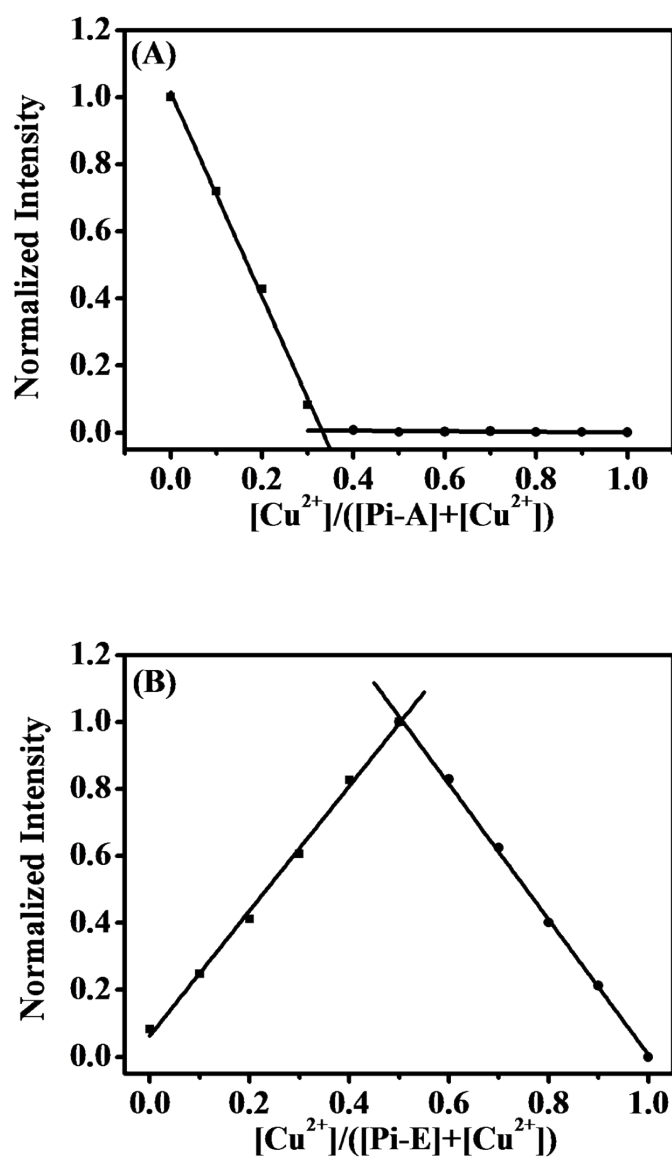


Fig. S8. (A) Job's plot of Pi-A and Cu^{2+} ($[\text{Pi-A}] + [\text{Cu}^{2+}] = 10 \mu\text{M}$) and (B) Job's plot of Pi-E and Cu^{2+} ($[\text{Pi-E}] + [\text{Cu}^{2+}] = 10 \mu\text{M}$). Buffer: Tris-HCl (10 mM, pH 7.4), 2% (v/v) DMSO/water.

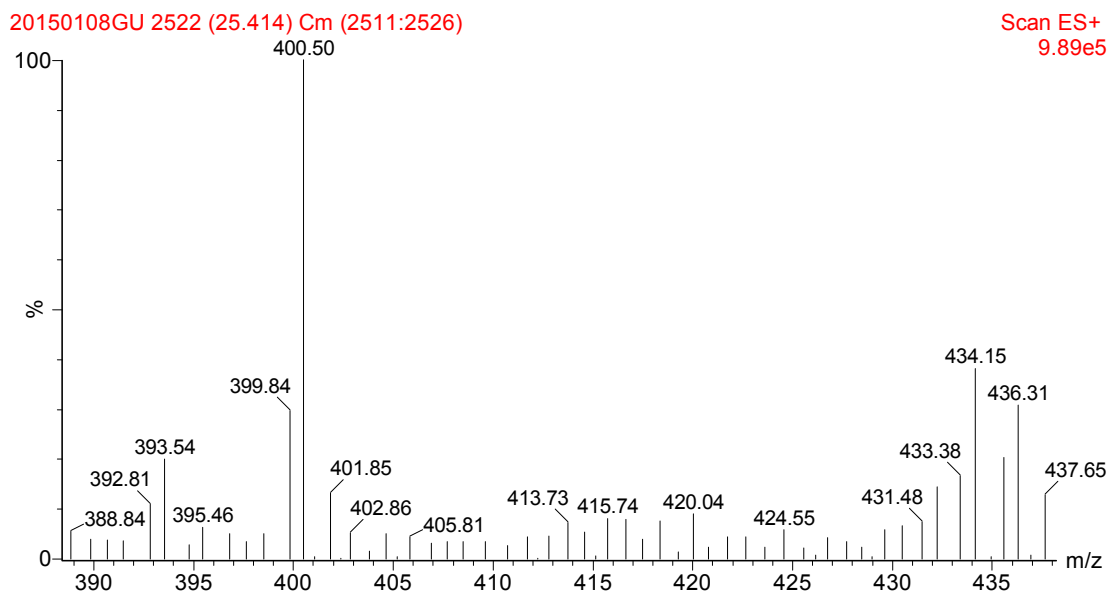


Fig. S9. ESI-MS spectrum of the reaction products of Pi-E with Cu²⁺.

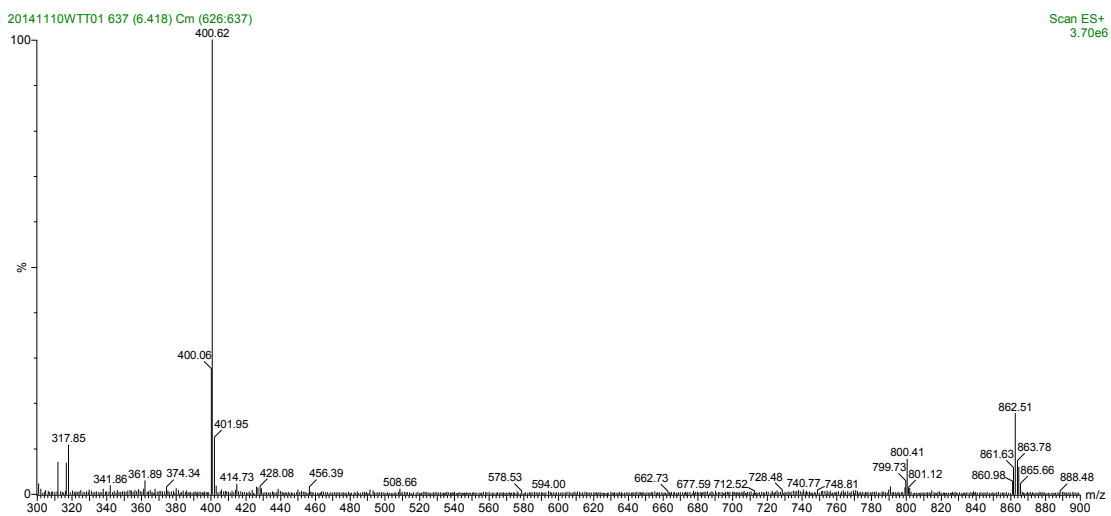


Fig. S10. ESI-MS spectrum of compound 2.

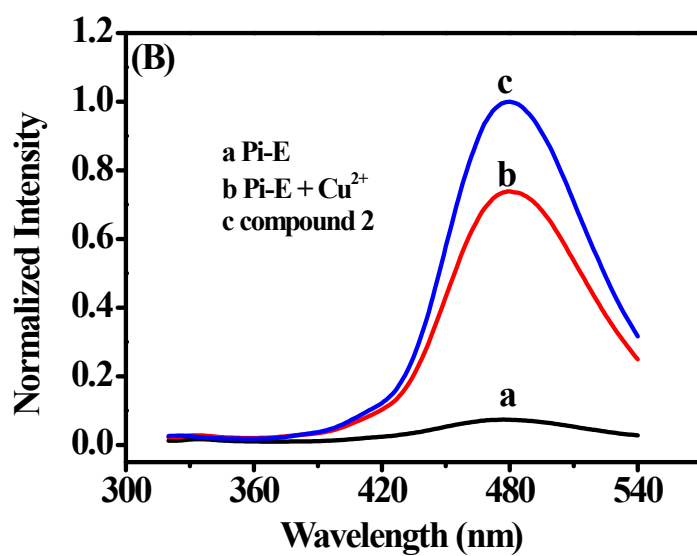
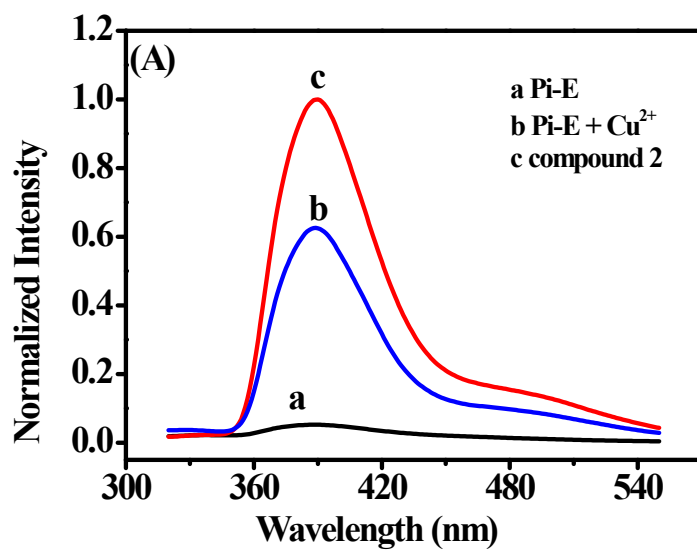
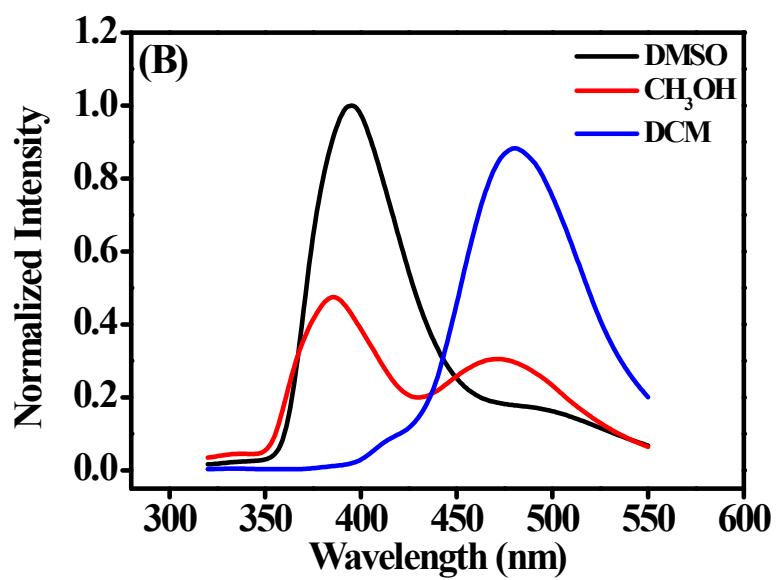
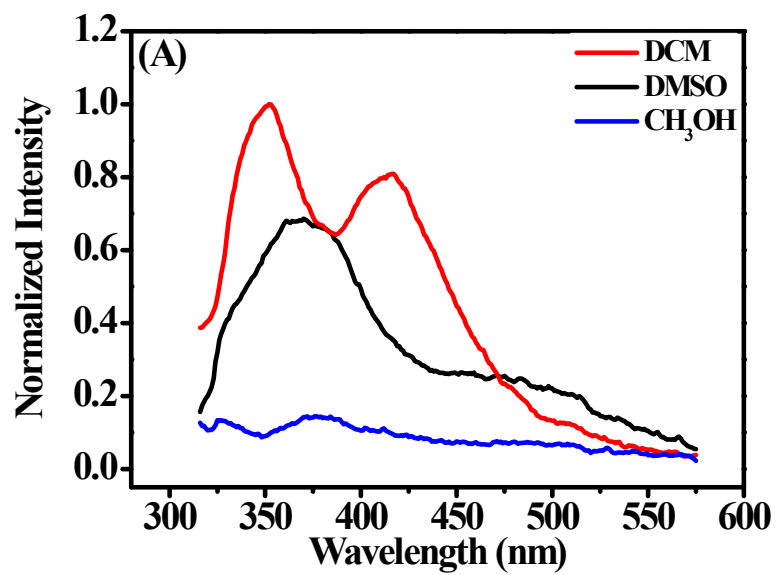


Fig. S11. Fluorescence spectra of 10 μ M Pi-E (a), 10 μ M Pi-E with 10 μ M Cu²⁺ (b) and 10 μ M compound 2 (c). Conditions: (A) in DMSO/Tris-HCl (v/v = 9:1) solution, $\lambda_{ex}/\lambda_{em}$ = 296/389 nm; (B) in DMSO/Tris-HCl (v/v = 1:49) solution at pH 7.4. $\lambda_{ex}/\lambda_{em}$ = 296/481 nm.



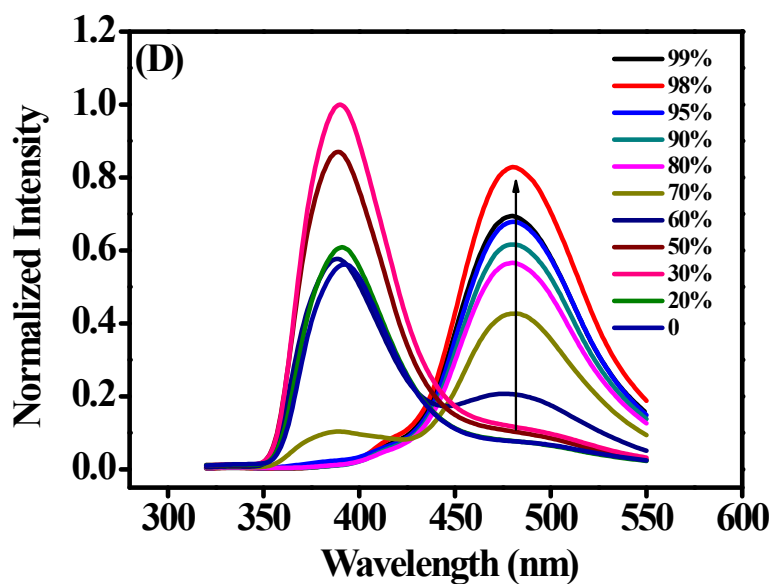
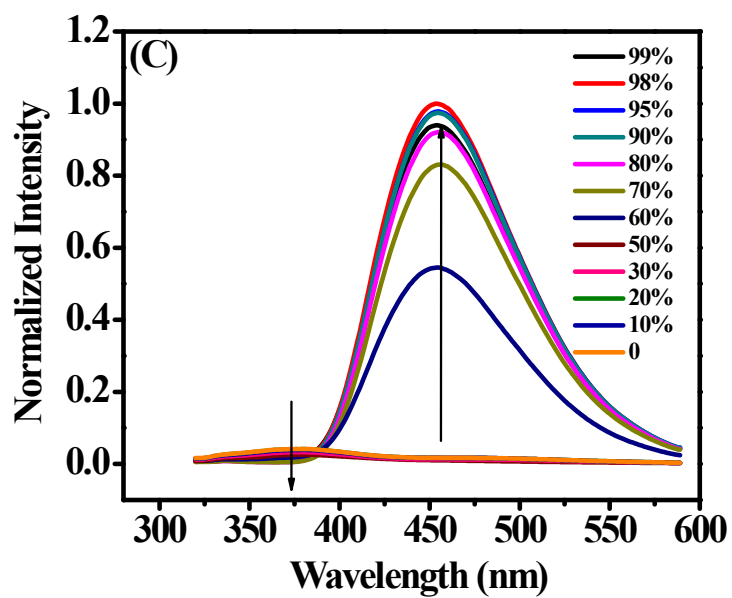


Fig. S12. Fluorescence spectra of 10 μM Pi-A (A) or compound **2** (B) in different solvents. Fluorescence spectra of 10 μM Pi-A (C) or compound **2** (D) in DMSO/water mixture of varying water proportions from 0 to 99%. $\lambda_{\text{exc}} = 296$ nm.

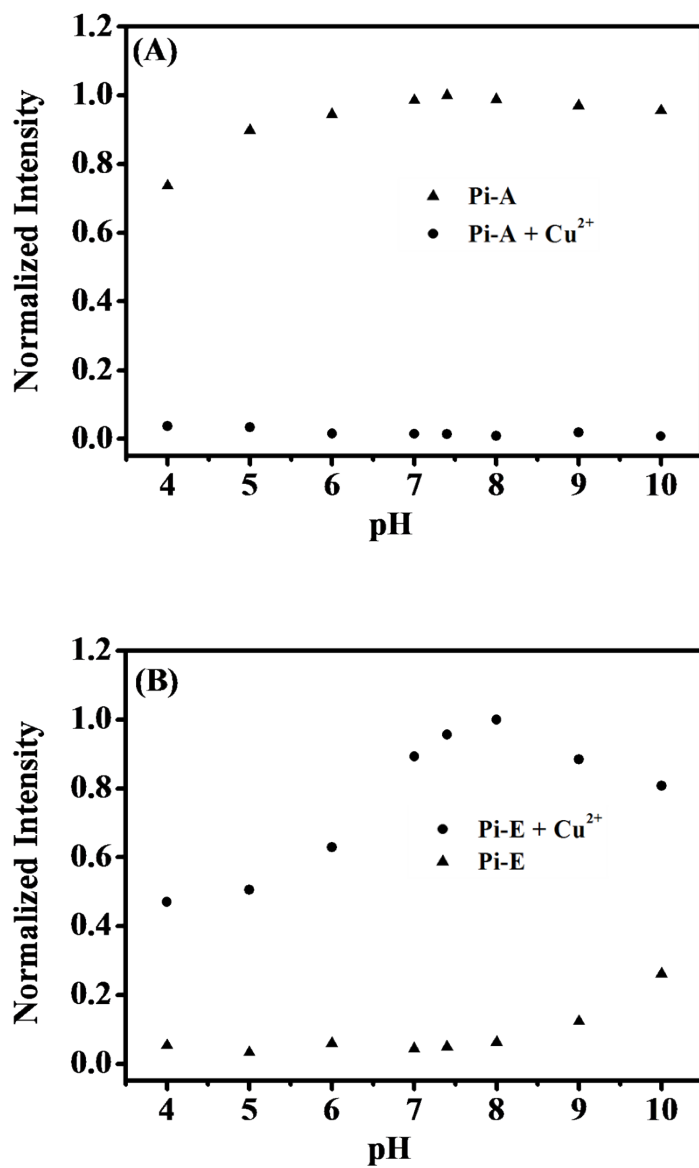


Fig. S13. Effect of pH on the fluorescence intensity of 10 μM Pi-A (A) and Pi-E (B) in the absence and presence of 10 μM Cu^{2+} . Buffer: 10 mM NaAc-HAc for pH 4.0-6.0 and 10 mM Tris-HCl buffer for pH 7.0-10.0. Conditions: for Pi-A, $\lambda_{\text{ex}}/\lambda_{\text{em}} = 296/455$ nm; for Pi-E, $\lambda_{\text{ex}}/\lambda_{\text{em}} = 296/481$ nm.

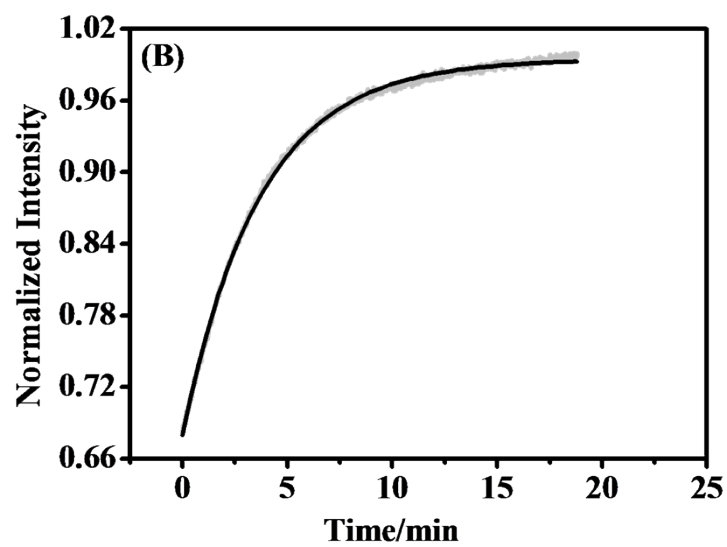
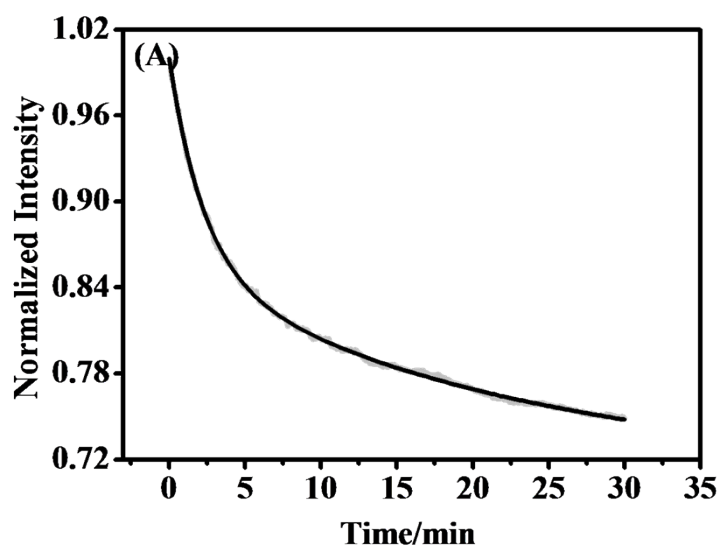


Fig. S14. Time-dependent fluorescence intensity of 10 μM Pi-A (A) and Pi-E (B) in the presence of 10 μM Cu^{2+} . Conditions: for Pi-A, $\lambda_{\text{ex}}/\lambda_{\text{em}} = 296/455$ nm; for Pi-E, $\lambda_{\text{ex}}/\lambda_{\text{em}} = 296/481$ nm. Buffer: Tris-HCl (10 mM, pH 7.4), 2% (v/v) DMSO/water. T= 25 °C.

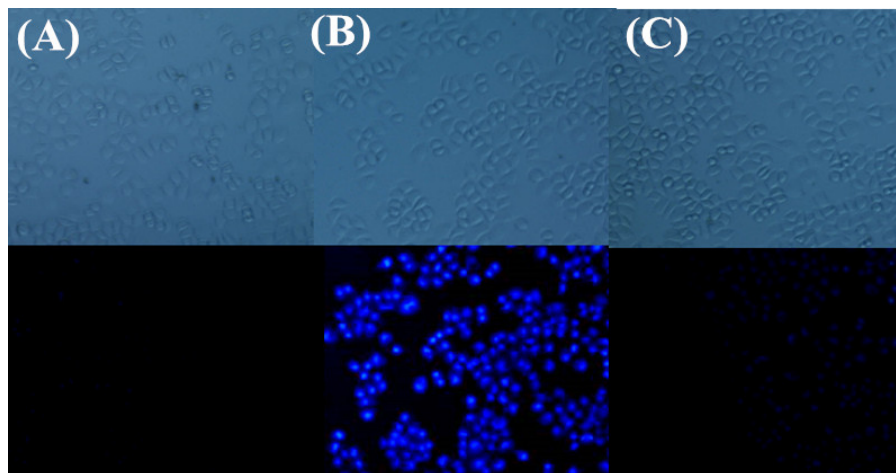


Fig. S15. Fluorescence microscope images of living HeLa cells. Cells incubated with PBS (A); 10 μ M Pi-A (B); 10 μ M Pi-E (C) for 30 min at 37 °C. Top: bright field image, Bottom: fluorescence image.